Cancer Research

Accumulation of MDSC and Th17 Cells in Patients with Metastatic Colorectal Cancer Predicts the Efficacy of a FOLFOX–Bevacizumab Drug Treatment Regimen

Emeric Limagne[1,2,3,4], Romain Euvrard[1,2], Marion Thibaudin[1,2], Cédric Rébé[1,2,3,4], Valentin Derangère[1,2,3,4], Angélique Chevriaux[1,2,3,4], Romain Boidot[1,2,3,4], Frédérique Végran[1,2,3,4], Nathalie Bonnefoy[5,6,7], Julie Vincent[3], Leila Bengrine-Lefevre[3], Sylvain Ladoire[1,2,3,4], Dominique Delmas[1,2], Lionel Apetoh[1,2,3], and François Ghiringhelli[1,2,3,4]

Abstract

Host immunity controls the development of colorectal cancer, and chemotherapy used to treat colorectal cancer is likely to recruit the host immune system at some level. Athough preclinical studies have argued that colorectal cancer drugs, such as 5-fluorouracil (5-FU) and oxaliplatin, exert such effects, their combination as employed in the oncology clinic has not been evaluated. Here, we report the results of prospective immunomonitoring of 25 metastatic colorectal cancer (mCRC) patients treated with a first-line combination regimen of 5-FU, oxaliplatin, and bevacizumab (FOLFOX–bevacizumab), as compared with 20 healthy volunteers. Before this therapy was initiated, T regulatory cells (Treg), Th17, and granulocytic myeloid-derived suppressor cells (gMDSC) were increased significantly in mCRC, but only a high level of gMDSC was associated with a poor prognosis. Chemotherapy modulated the Treg/Th17 balance by decreasing Treg and increasing Th17 cell frequency by 15 days after the start of treatment. Increased Th17 frequency was associated with a poor prognosis. FOLFOX–bevacizumab treatment elicited a decrease in gMDSC in 15 of 25 patients and was associated with a better survival outcome. Notably, the gMDSCs that expressed high levels of PD-L1, CD39, and CD73 exerted a robust immunosuppressive activity, relative to other myeloid cells present in blood, which could be reversed by blocking the CD39/CD73 and PD-1/PD-L1 axes. Our work underscores the critical prognostic impact of early modifications in Th17 and gMDSC frequency in mCRC. Furthermore, it provides a clinical rationale to combine FOLFOX–bevacizumab chemotherapy with inhibitors of ATP ectonucleotidases and/or anti-PD-1/PD-L1 antibodies to more effectively treat this disease. *Cancer Res; 76(18); 5241–52. ©2016 AACR.*

Introduction

Colorectal cancer is the fourth most commonly diagnosed cancer worldwide and is a major cause of cancer-related deaths. Numerous studies have demonstrated a link between chronic inflammation and many cancers, including colorectal cancer. For example, inflammatory bowel disease is associated with increased incidence of colorectal cancer (1). Colorectal cancer is controlled by the immune system: Accumulating evidence shows that T-cell infiltration of primary tumors is associated with better prognosis (2, 3). Similar findings were also observed in patients with metastatic colorectal cancer (mCRC; ref. 4). In particular, infiltration with memory CD8 T cells, follicular helper T cells, or regulatory T cells (Treg) is associated with better tumor prognosis in colorectal cancer (5–7). However, infiltration with Th17 cells is associated with poor prognosis (8) due to the secretion of proinflammatory cytokines like IL17A, which can promote angiogenesis or other protumor effects (9).

Myeloid-derived suppressor cells (MDSC) are a heterogeneous population composed of myeloid cells blocked at several stages of differentiation. These cells were observed to accumulate in the blood, lymph nodes, bone marrow, and tumor sites of tumor-bearing patients and in experimental animal models of cancer (10, 11). These cells are characterized by their ability to inhibit both innate and adaptive immune responses, thus having a negative effect on antitumor immunity (12). In humans, MDSCs are not well characterized, partially because no unified markers are currently available for these cells. However, these cells typically express the common myeloid markers, CD33 and CD11b, but lack markers of mature myeloid cells, such as HLA-DR. Among human MDSCs, the monocytic subset comprises $CD14^+$ cells, and

[1]INSERM, U866, Dijon, France. [2]UFR des Sciences de Santé, Université de Bourgogne-Franche Comté, Dijon, France. [3]Centre Georges François Leclerc, Dijon, France. [4]Plateforme de Transfert en Biologie Cancérologique, CGFL, Dijon, France. [5]Institut de Recherche en Cancérologie de Montpellier, Montpellier, France. [6]INSERM U1194, Université de Montpellier, Montpellier, France. [7]OREGA Biotech, Ecully, France.

Note: Supplementary data for this article are available at Cancer Research Online (http://cancerres.aacrjournals.org/).

E. Limagne and R. Euvrard share first authorship of this article.

L. Apetoh and F. Ghiringhelli share senior authorship of this article.

Corresponding Authors: Emeric Limagne, Centre Georges-François Leclerc, 1 rue du Pr Marion, Dijon 21000, France. Phone: 038-039-3383; Fax: 038-039-3434; E-mail: elimagne@cgfl.fr; and François Ghiringhelli, fghiringhelli@cgfl.fr

doi: 10.1158/0008-5472.CAN-15-3164

the granulocytic subset comprises $CD15^+$ cells (13, 14). We previously reported that 5-fluorouracil (5-FU) could induce MDSC depletion in mouse models of cancer (15) but enhance Th17 cell accumulation (15, 16).

Currently, mCRC patients are frequently treated in front line with a combination of chemotherapies, which associates 5-FU with either oxaliplatin (FOLFOX) or irinotecan (FOLFIRI). In addition to the chemotherapeutic regimens, patients are often treated with biotherapies, such as antiangiogenic agents like the anti-VEGF mAb bevacizumab or anti-EGFR mAb. The effect of such combination chemotherapies on peripheral immune responses is currently poorly explored. In addition, the prognostic value of initial immune parameters and their putative alteration by chemotherapy is also unknown.

In this work, we have first compared blood repartition of memory T-helper cells and MDSC [granulocytic MDSC (gMDSC) and monocytiic MDSC (mMDSC)] subsets in 20 healthy volunteers versus 25 consecutive mCRCs treated with FOLFOX plus bevacizumab combination as first line and tested the association of immune parameters with patients' outcome.

Patients and Methods

Patients and healthy donors

Between January 2014 and October 2014, we collected whole blood from healthy volunteers ($n = 20$) and mCRC patients ($n = 25$) at the Centre Georges François Leclerc (Dijon, France). mCRC patients were diagnosed in our cancer center and were proposed to be treated with FOLFOX plus bevacizumab as a first-line regimen. FOLFOX regimen was given every 14 days as follows: oxaliplatin (85 mg/m^2 over 2 hours), leucovorin (400 mg/m^2 over 2 hours), and 5-FU (400 mg/m^2 bolus, then 2,400 mg/m^2 over 46 hours). Bevacizumab was given at a dose of 5 mg/kg once every 2 weeks.

After 12 cycles or sooner in case of toxicity, responder patients received a maintenance treatment with bevacizumab, leucovorin (400 mg/m^2 over 2 hours), and 5-FU (400 mg/m^2 bolus, then 2,400 mg/m^2 over 46 hours every 2 weeks). All patients must have received at least four cycles of chemotherapy to be evaluable. Tumor response was prospectively assessed every four cycles according to RECIST criteria by CT scan (17). Treatment was repeated until the occurrence of disease progression or unacceptable toxicity, whichever occurred first.

Validation set

We added another study of immunomonitoring performed on 20 patients treated in Centre Georges François Leclerc for mCRC in second or third line by 5-FU–based chemotherapy plus bevacizumab combination.

All patients gave informed consent approved by the local Ethics Committee. The collection of blood sample is authorized by the French authorization (nr. AC2014-2460). No additional blood samples beyond those required for routine testing were taken. Whole blood of mCRC patients was sampled before (D0) and after chemotherapy (D15, D30, and D60) on EDTA-K2 tubes (BD Biosciences) for complete blood count, which was performed in our Clinical Biology Unit (Centre George François Leclerc) and on heparinized tube for leucocyte phenotyping. All analyses were performed following the first 6 hours after sampling. Review of pathology reports confirmed the diagnosis. Information regarding clinical, pathologic, and biological characters of patients and healthy volunteers is presented in Supplementary Table S1.

Flow cytometry

Antibodies and cytometry procedure. Anti-CXCR3-PE-Vio700 (REA232), anti-CCR6-PE (REA190), anti-CD25-APC (4E3), anti-CD45RA-APV-Vio770 (T6D11), anti-CD4-VioGreen (VIT4), anti-CD8-VioGreen (BW135/80), anti-CD33-APC-Vio770 (AC104.3E3), anti-HLA-DR-Vioblue (AC122), anti-CD15-Vio-Green (VIMC6), anti-CD14-PerCP-Vio700 (TUK4), anti-CD3-FITC (BW264/56), anti-CD56-FITC (REA136), anti-CD19-FITC (LT19), anti-CD20-FITC (LT20), anti-TNF-α–PE (REA656), and anti-Foxp3-PE (3G3) were purchased from Miltenyi Biotec. Anti-CCR4-BV450 (1G1), anti-PD-L1-APC (MIH1), anti-Ki-67-eFluor450 (20Raj1), and anti-PD-1-PerCP-eFluor710 (J105) were purchased from BD Biosciences and eBioscience, respectively. Anti-CD4-Alexa Fluor 700 (RPA-T4), anti-CD39-PE (A1), anti-CD73-Brillant Violet 421 (AD2), and anti-IL17A-Pacific Blue (BL168) were purchased from BioLegend. All events were acquired by a BD LSR-II cytometer equipped with BD FACSDiva software (BD Biosciences), and data were analyzed using FlowJo software (Tree Star).

Leucocyte population identification and numeration. For leucocytes identification by flow cytometry, whole blood removed to heparinized tube (100 μL) was stained with different antibody cocktail for 45 minutes at room temperature. For MDSC identification, we used lineage cocktail (CD3, 56, 19, and 20), CD33, CD15, CD14, and HLA-DR antibody. For Treg analysis, we used CD4, CD45RA, CD25, and Foxp3 antibodies, and for other T-helper subsets, we used CD4, CD45RA, CD25, CCR6, CXCR3, and CCR4 antibodies. The gating strategy is described in Supplementary Fig. S1 and S2. After surface staining, 2 mL of red blood cells lysis solution (BD Biosciences) was added for 10 minutes, centrifuged (400 × *g*, 5 minutes), and then resuspended in flow cytometry buffer (eBioscience). Foxp3 staining was carried out according to the manufacturer's protocol using the fixation/permeabilization solution (eBioscience).

Suppression assays

To test MDSC subset suppressive activity, total $CD3^+$ lymphocytes and MDSC subsets were sorted from mCRC patient blood (around 15 mL). For gMDSC and granulocytes isolation (around 7.5 mL of blood), we used Whole Blood CD15 MicroBeads and column following the manufacturer's instructions (Miltenyi Biotec). For mMDSC and monocytes isolation (around 7.5 mL of blood), we performed peripheral blood mononuclear cell (PBMC) isolation on lymphocyte separation medium (Eurobio). $CD15^+$ cells and PBMCs were then stained with anti-CD33-APC-Vio770 (AC104.3E3), anti-HLA-DR-Vioblue (AC122), anti-CD15-VioGreen (VIMC6), anti-CD14-PerCP-Vio700 (TUK4), and anti-CD3-FITC (BW264/56) in flow cytometry buffer (eBioscience) for 30 minutes. Myeloid subsets (gMDSC, mMDSC, monocytes, and granulocytes) and total T cells were cell sorted on ARIA-III (BD Biosciences). $CD3^+$ cells were activated with 2 μg/mL anti-CD3 (Bio X Cell) and anti-CD28 (Bio X Cell) as effector cells and cocultured with or without gMDSC, mMDSC, granulocytes, or monocytes (T-cell/myeloid cell ratios are 10:1 or 25:1) for one week in culture medium (AIM V Medium, Fisher Scientific) in the presence of 2 μmol/L of ATP (Sigma). In some experiments, the CD39-neutralizing antibody

(OREGA Biotech, clone BY40, 10 μg/mL) and/or anti-PD-1 antibody (Nivolumab, 2 μg/mL) were added. In some experiments, TNFα and Ki67 expression was assessed in $CD3^+$ T cells by flow cytometry after 24 hours of coculture with or without MDSCs. This was performed in the presence of anti-CD3 (2 μg/mL, Bio X Cell) and anti-CD28 (2 μg/mL, Bio X Cell). Mouse IgG1 (11711, R&D Systems) and human IgG4 (ET904, eBioscience) antibodies were respectively used as a control for anti-CD39 and anti-PD-1 antibody efficacy.

Measurement of cytokines

After 5 days of culture, cell culture supernatants were assessed by ELISA for human TNFα (Biolegend) according to the manufacturer's protocol.

For intracellular cytokine staining, cells were stimulated for 4 hours at 37°C in culture medium containing PMA (50 ng/mL; Sigma-Aldrich), ionomycin (1 μg/mL; Sigma-Aldrich), and monensin (GolgiStop; 1 μL/mL; BD Biosciences). After staining for surface markers [anti-CD3-FITC (BW264/56)], cells were fixed and permeabilized according to the manufacturer's instructions (Fixation/Permeabilization Kit; eBiosciences), then stained for intracellular products. Antibodies used for intracellular staining were as follows: phycoerythrin (PE)-conjugated anti-TNFα or eFluor 450–conjugated anti-Ki67.

qRT-PCR

Total RNA from T cells was extracted with TRI Reagent (Ambion), reverse transcribed using M-MLV Reverse Transcriptase (Invitrogen), and was analyzed by qRT-PCR with the SYBR Green method according to the manufacturer's instructions using the 7500 Fast Real Time PCR System (Applied Biosystems). Expression was normalized to the expression of human *ACTB*. Primers designed to assess gene expression are as reported in Supplementary Table S2.

Statistical analyses

For the analysis of data, comparison of continuous data was achieved by the Mann–Whitney U test or Wilcoxon Test and comparison of categorical data by Fisher exact test, as appropriate. All P values are two tailed. $P < 0.05$ was considered significant. Data are represented as mean ± SEM. All patients were followed up until death or the end of data recording (May 30, 2015). Progression-free survival (PFS) was calculated from the date when therapy started to the date of disease progression, and overall survival was calculated from the date when therapy started to the date of death. Median follow-up with its 95% confidence interval (CI) was calculated using the reverse Kaplan–Meier method. Survival probabilities were estimated using the Kaplan–Meier method, and survival curves were compared using the log-rank test. Analyses were performed using MedCalc Software.

Determination of the required number of patients

We proposed to separate patients using median as a cutoff to have comparable number of patients in the two groups. The rate of PFS under FOLFOX–bevacizumab is about 60% at 6 months (18). We decided to only foster on clinically relevant biomarker that could separate a group of patients with 6 months PFS rate of 40% versus 80%. With a risk α of 5% and a power of 80%, we needed a minimum of 11 patients per group to detect a difference. For this reason, we decided to include 25 patients.

Results

Accumulation of Treg and Th17 and Th1 depletion in mCRC patients

We first analyzed the frequency of circulating immune cell populations from mCRC patients at baseline compared with healthy individuals. The clinical characteristics and blood parameters of patients and healthy volunteers are summarized in Supplementary Table S1 and Supplementary Fig. S3. To assess the frequency of memory T-cell subpopulations, we relied on their chemokine receptor expression using a gating strategy adapted from Mahnke and colleagues (19). The transcription factor Foxp3 occurred with a concomitant high expression of CD25, while Th1, Th2, Th17, and Th17/Th1 cells were analyzed on the basis of their expressions of CCR6, CXCR3, and CCR4 (Supplementary Fig. S1). To validate our gating strategy, we analyzed IFNγ and IL17A cytokine expressions in memory T-CD4 cells regarding chemokine receptor expression (Supplementary Fig. S4). The frequency of memory Th2 cells was comparable between healthy volunteers and mCRC patients while there was a small decrease in memory Th1 ($P = 0.035$) in mCRC (Fig. 1A). In contrast, we observed a significant increase in the number of Treg ($P < 0.0001$) and Th17 cells ($P = 0.019$) while inflammatory Th17 cells expressing the CXCR3 marker, and called Th17/Th1 in the article, did not accumulate in mCRC patients ($P = 0.071$) (Fig. 1A). We then studied the prognostic role of accumulation of Treg or Th17 cells. We separated patients into two groups using median as a cutoff, and we did not observe any association between Treg ($P = 0.68$) or Th17 ($P = 0.42$) accumulation and PFS during first-line chemotherapy and overall survival (Fig. 1B and C and not shown). Th1, Th2, and inflammatory Th17 cells were also not associated with prognosis (not shown). Together, these data show alterations in the frequency of memory T-helper populations in mCRC patients compared with healthy donors. However, these changes do not seem to affect tumor prognosis.

Effect of FOLFOX–bevacizumab regimen on subsets of memory CD4 T cells

Chemotherapy using 5-FU was shown to affect both MDSC levels and T-cell polarization (15, 16). Oxaliplatin was also shown to improve antitumor T-cell functions via a mechanism called immunogenic cell death (20). We observed that one cycle of chemotherapy did not significantly alter the number of circulating lymphocytes (Supplementary Fig. S5). T-helper frequencies (Th1, Th2, Treg, Th1/Th17, and Th17) were monitored at days 0, 15, 30, and 60 after chemotherapy. In the 25 mCRC patients, we did not observe any change in the frequency of Th1, Th2, and Th17/Th1. For Treg and Th17 cells, we observed only a respective decrease ($P = 0.013$) and increase ($P = 0.047$) frequency at day 15 that did not persist during follow-up (Fig. 2A). As a control, we could not detect significant modification of Treg and Th17 frequencies in untreated patients (data not shown). Importantly, when we focused on the impact of modifications of memory CD4 T-helper cell frequency on PFS, we observed a subset of patients whose Treg number is decreased 15 days after the first cycle of chemotherapy. This modulation is maintained during the whole follow-up (D30, $P = 0.021$; D60, $P = 0.013$). Nevertheless, Treg frequency modulation at day 15 was not associated with PFS ($P = 0.42$; Fig. 2B and C). Concerning Th17 cells' frequency modulation, we also observed a subset of patients whose Th17 percentage increased 15 days after the first cycle of chemotherapy. This increase is only

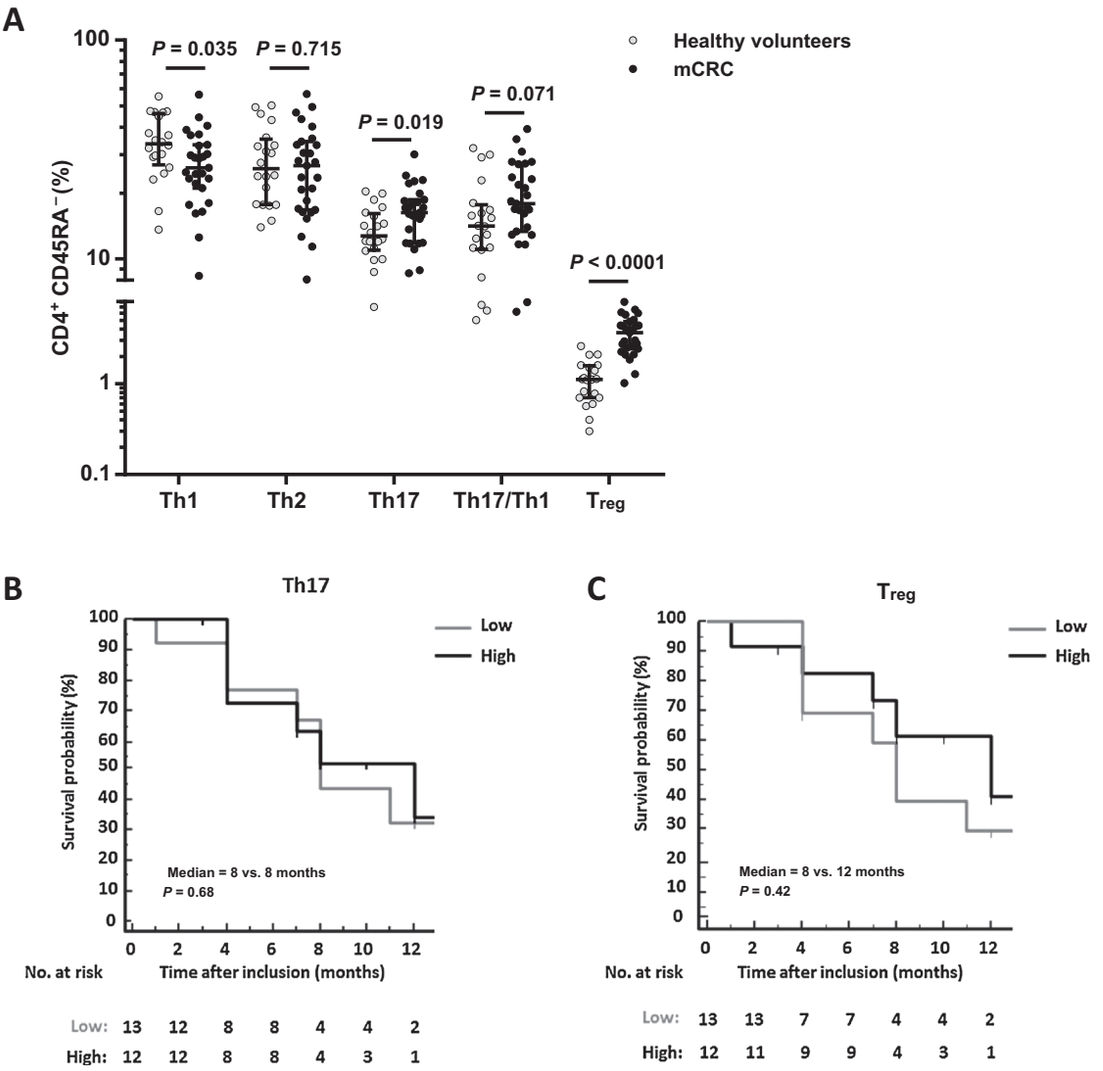

Figure 1.

Treg, Th17 accumulation, and Th1 depletion in mCRC patients. **A,** whole blood of healthy volunteers or mCRC patients was stained with anti-CD4, anti-CD45RA, anti-CCR6, anti-CXCR3, anti-CCR4, anti-CD25, and anti-Foxp3 antibodies and analyzed by flow cytometry. The frequency of memory CD4 (CD45RA$^-$ CD4$^+$), Th1 (CCR6$^-$ CXCR3$^+$), Th2 (CCR6$^-$ CXCR3$^-$ CCR4$^+$), Th17 (CCR6$^+$ CXCR3$^-$), Th17/Th1 (CCR6$^+$ CXCR3$^+$), and Treg (CD25^{high} Foxp3$^+$) cells is depicted. The data presented constitute the analyses performed on 20 healthy volunteers and 25 mCRC patients. **B,** Kaplan–Meier curve of PFS for patients with mCRC according to the presence of a high or low level of Th17 cells in blood (using median frequency as a cutoff). **C,** Kaplan–Meier curve of PFS for patients with mCRC according to the presence of a high or low level of Treg cells in blood (using median frequency as a cutoff).

transitory. However, this increase in Th17 cell frequency at day 15 was associated with a poor PFS ($P = 0.048$; Fig. 2D and E). In the group of patients with increased Th17 frequency, we observed 46% of partial response after 3 months of treatment, while all patients presented a partial response upon RECIST criteria in the group of patients with a decrease of Th17 cell frequency ($P = 0.03$, Fisher exact test). We could observe similar prognostic role of Th17 frequency decrease after a cycle of 5-FU–based chemotherapy plus bevacizumab in a series of 20 metastatic colorectal cancer patients treated by this protocol in second or third line [median PFS of 7 months vs. 4 months for patients with decreased vs. increased Th17 frequency ($P = 0.04$; data not shown)]. Together, these results show that after the first cycle of chemotherapy, Treg frequency decreased to a normal level while Th17 frequency increased in some patients. Increased Th17 level is associated with poor prognosis and resistance to therapy.

Accumulation of MDSCs in mCRC patients

We also investigated the frequency of MDSCs using the Lin$^-$ CD33^{high} HLA-DR$^-$ cell labeling. Using CD14 and CD15 labeling, we separated the two types of MDSCs: gMDSCs, which express CD15 and CD14 marker; and mMDSCs, which express the CD14 marker only (Supplementary Fig. S2). To validate our gating strategy, we cell sorted from mCRC whole-blood CD15$^+$ cells using magnetic beads. These cells were then separated cells upon CD33 labeling and we observed that only CD15$^+$ CD33^{high}

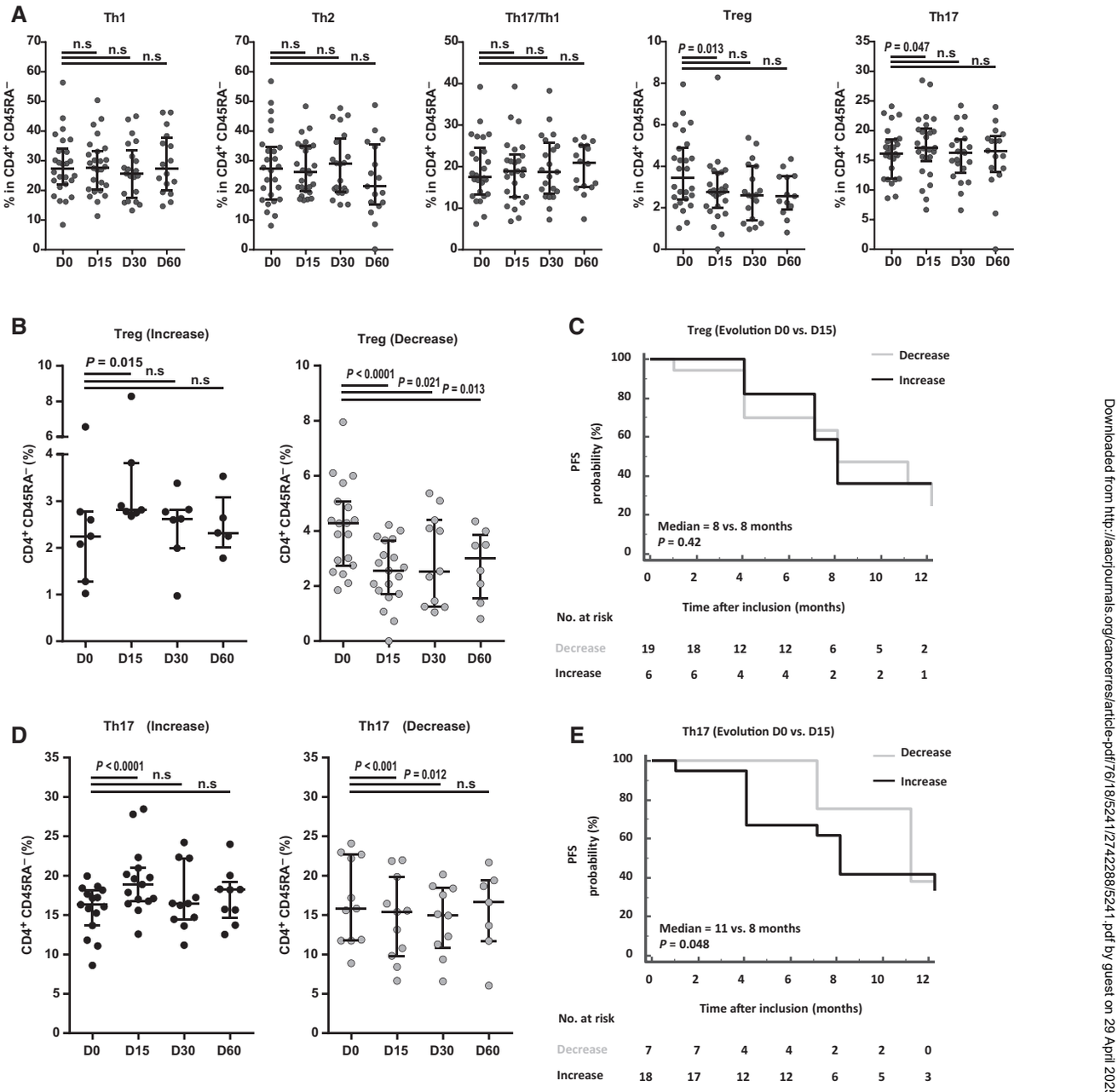

Figure 2.

Effect of FOLFOX–bevacizumab regimen on memory CD4 T-cell subsets. **A,** whole blood of mCRC patients was stained with anti-CD4, anti-CD45RA, anti-CCR6, anti-CXCR3, anti-CCR4, anti-CD25, and anti-Foxp3 antibodies and was analyzed by flow cytometry before (D0) and after (D15, D30, and D60) first-line chemotherapy. Memory CD4 T-cell frequency is depicted as described in Fig. 1. The data presented constitute the analyses performed on 25 mCRC patients. **B,** evolution (D0, D15, D30, and D60) of Treg cell frequency in the blood of a patient with an induction or a decrease of Treg after chemotherapy (D0 vs. D15). **C,** Kaplan–Meier curve of PFS for patients with mCRC according to the evolution (increase vs. decrease) of Treg cell frequency in blood before (D0) and after (D15) chemotherapy. **D,** evolution (D0, D15, D30, and D60) of Th17 cell frequency in the blood of a patient with an induction or a decrease of Th17 after chemotherapy (D0 vs. D15). **E,** Kaplan–Meier curve of PFS for patients with mCRC according to the evolution (increase vs. decrease) of Th17 cell frequency in blood before (D0) and after (D15) chemotherapy. n.s., not significant.

cells exerted immunosuppressive function and could be called gMDSCs, while $CD15^+$ $CD33^{low}$ cells did not exert suppressive function and could be called granulocytes (Fig. 3A–C). For $CD14^+$ cells isolated from PBMC, all cells expressed CD33 labeling but only cells with HLA-DR^{low} expression had immunosuppressive function and could be called mMDSCs (Fig. 3A–C). In addition, only $CD15^+$ $CD33^{high}$ gMDSCs but not $CD15^+$ $CD33^{low}$ granulocytes expressed CD124 (IL4Rα), a classical marker of MDSC

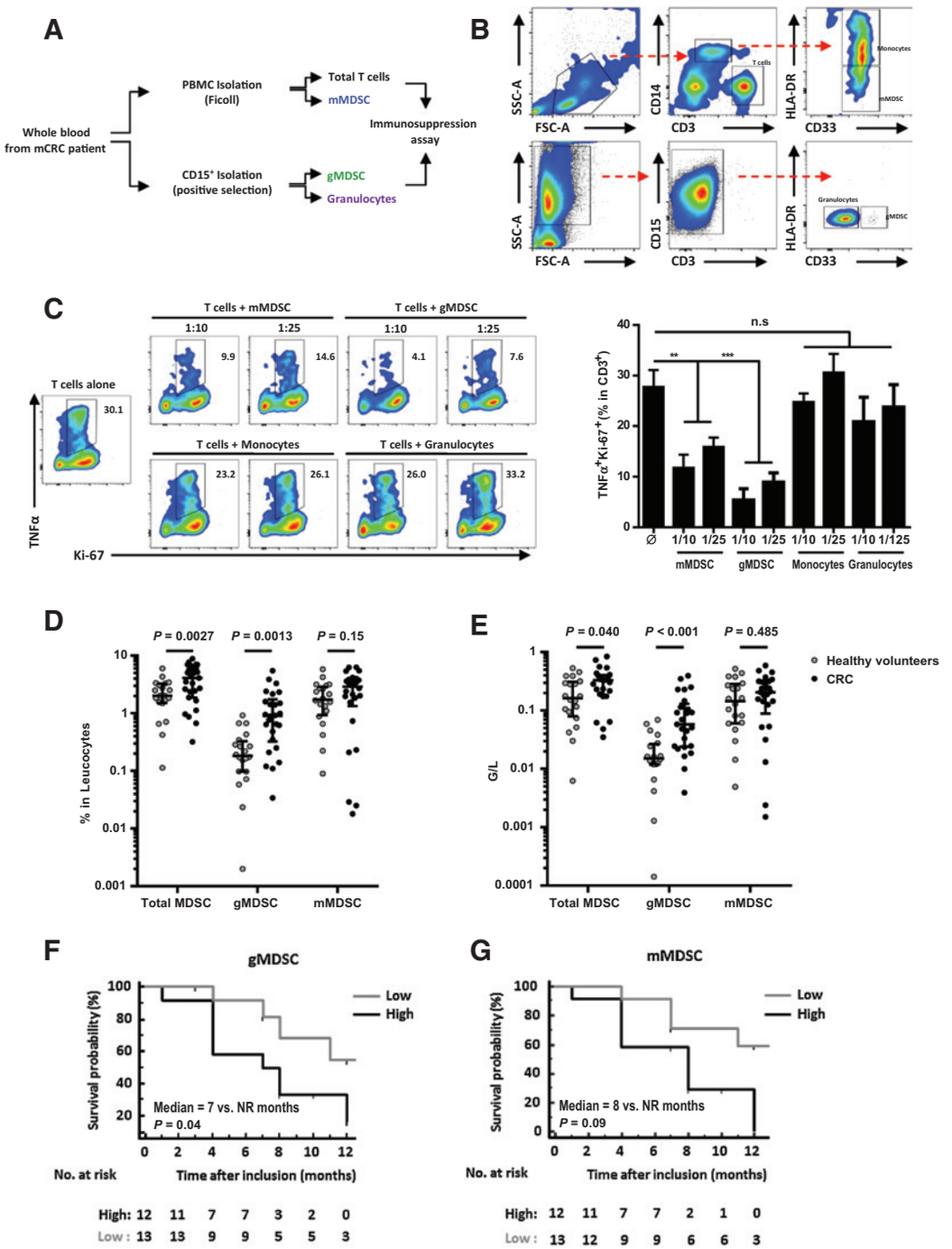

Figure 3.

Accumulation of MDSCs in mCRC patients. **A,** graphical representation of cell-sorting experiment performed for analysis of MDSC, monocyte, and granulocyte-suppressive capacities on autologous T cells. **B,** representative gating strategy used for T cells, mMDSC, granulocytes, and gMDSC sorting from an mCRC patient's whole blood. **C,** total $CD3^+$ lymphocytes, granulocytes, and gMDSC subsets were sorted from a cancer patient's blood. Then, $CD3^+$ T cells were activated with anti-CD3 and anti-CD28 as effector cells and cocultured (in the presence of ATP) with or without myeloid cells at different ratios (1:10 or 1:25, myeloid cells: T cells) during 5 days. We usually used around 20,000 T cells in our immunosuppression assay. TNFα and Ki67 expressions were assessed using intracellular staining and were analyzed in $CD3^+$ T cells. One representative experiment is shown ($n = 3$ mCRC patients). n.s., not significant. **D** and **E,** whole blood of healthy volunteers or mCRC patients was stained with anti-CD33, anti-Lin (i.e., anti-CD3, -CD19, -CD20, -CD56), anti-HLA-DR, anti-CD14, and anti-CD15 antibodies and was analyzed by flow cytometry. The frequency (**D**) or the absolute count (**E**) of gMDSC ($CD33^+$ Lin^- HLA-$DR^{-/low}$ $CD14^-$ $CD15^+$) or mMDSC ($CD33^+$ Lin^- HLA-$DR^{-/low}$ $CD14^+$ $CD15^-$) is depicted. The data presented constitute the analysis performed on 20 healthy volunteers and 25 mCRC patients. **F,** Kaplan–Meier curve of PFS for patients with mCRC according to the presence of a high or low level of gMDSC cells in blood (using median frequency as a cutoff). **G,** Kaplan–Meier curve of PFS for patients with mCRC according to the presence of a high or low level of mMDSC cells in blood (using median frequency as a cutoff).

(Supplementary Fig. S2D). The proportion and absolute number of total MDSCs in peripheral blood from untreated mCRC patients was significantly increased compared with the proportion found in healthy donors ($P = 0.0027$; Fig. 3D). We also observed that both the frequency (Fig. 3D) and the absolute number (Fig. 3E) of gMDSC ($P = 0.0013$ and $P < 0.001$), but not mMDSC ($P = 0.15$ and $P = 0.485$), significantly accumulate in the blood of mCRC patients compared with healthy donors. We then studied the prognostic role of MDSCs. As described above, we separated patients into two groups using median MDSC frequency as a cutoff. We observed that high levels of gMDSC at baseline are significantly associated with poor PFS [7 months vs. median not reached (NR), $P = 0.04$] and overall survival (12 months vs. 23 months, $P = 0.04$; data not shown), while mMDSC level is not associated with prognosis (Fig. 3F and G). We also confirmed that decrease in the frequency of gMDSC is significantly associated with longer median PFS after a cycle of 5-FU–based chemotherapy plus bevacizumab in a series of 20 colorectal patients treated by this protocol in second or third line [median PFS 6 months vs. 4 months for patients with decreased vs. increased gMDSC frequency ($P = 0.05$; data not shown)]. Together, these data show that mCRC patients have high levels of MDSCs, and initial high levels of gMDSCs are associated with poor prognosis.

Effect of FOLFOX–bevacizumab regimen on MDSC frequency

We previously observed that 5-FU induced MDSC cell death in humans, so we tested the effect of the first cycle of FOLFOX–bevacizumab chemotherapy on the frequency of MDSCs. We tested the evolution of MDSC frequency during the first 2 months of treatment. We observed that FOLFOX–bevacizumab chemotherapy did not impact on total MDSC or mMDSC frequency. In contrast, we observed a significant decrease in the number of gMDSCs 2 months after the beginning of the treatment ($P = 0.008$; Fig. 4A). As a control, we could not detect significant modification of MDSC frequency in untreated patients (data not shown). However, when we studied gMDSC, we found that 15 of 25 patients have a decreased frequency of gMDSC after the first cycle of chemotherapy compared with baseline (Fig. 4B). Analysis of gMDSC frequency at days 30 and 60 after initiation of the treatment confirmed that decreased frequency of gMDSC is maintained during the whole follow-up. For the other 10 patients, we did not observe a decrease in gMDSC frequency. Importantly, we observed that decrease in the gMDSC frequency is significantly associated with better prognosis and longer PFS ($P = 0.006$; Fig. 4C). In contrast for mMDSC, we observed that patients with a decreased frequency of mMDSC at day 15 did not maintain this evolution during the whole follow-up (D30, $P = 0.57$; D60, $P = 0.99$). Patients with an increased frequency of mMDSC at day 15 maintained this evolution during the whole follow-up (D30, $P = 0.0013$; D60, $P = 0.006$; Fig. 4D). The increase of mMDSC frequency did not change PFS ($P = 0.09$; Fig. 4E). We also confirmed that decrease in the frequency of gMDSC is significantly associated with longer median PFS after a cycle of 5-FU–based chemotherapy plus bevacizumab in a series of 20 metastatic colorectal cancer patients treated by this protocol in second or third line [median PFS 6 months vs. 4 months for patients with decreased vs. increased gMDSC frequency ($P = 0.05$; data not shown)]. Together, these data show that FOLFOX–bevacizumab induces a decrease of gMDSC, and this decrease is associated with better PFS.

MDSCs in mCRC patients express high levels of CD73, CD39, and PD-L1

Previous reports suggested that MDSCs in human cancers could suppress immunity using PD-L1 and CD39 (14, 21). PD-L1 interacts with PD-1, which is located on the surface membrane of effector memory T cells, and transmits an inhibitory signal reducing the proliferation and activity of these cells. CD39 is an ectonucleotidase that converts extracellular ATP or ADP into AMP. CD39 works together with CD73, another ectonucleotidase that converts AMP into adenosine, which is the final immunosuppressive molecule (22). Thus, both enzymes are required to convert ATP into the immunosuppressive molecule adenosine. We first tested the expression of PD-L1, CD73, and CD39 in the peripheral different myeloid cells (gMDSC and mMDSC, granulocytes, and monocytes) of mCRC patients and healthy volunteers. We observed that gMDSC is the myeloid population that expressed the highest levels of PD-L1, CD73, and CD39 (Fig. 5A–C). Interestingly, a higher expression of PD-L1, CD39, and CD73 is observed in gMDSCs of mCRC patients compared with healthy volunteers, thus suggesting a more important immunosuppressive activity in mCRC patients (Fig. 5A–C). We also confirmed that gMDSC of mCRC patients expressed more *Pdl1*, *Entpd1*, and *Nt5e* (coding for CD39 and CD73, respectively) mRNA than mMDSC (Supplementary Fig. S6).

To exert its immunosuppressive effect, PD-L1 must encounter PD-1 on a T cell. We checked the level of expression of PD-1 in CD4 and CD8 T-cell subsets of mCRC patients and observed a high expression of PD-1 on memory CD8 T cells in both healthy volunteers and mCRC patients. In CD4 T cells, PD-1 is only found on Th1 cells and a higher level is found in mCRC patients compared with healthy volunteers (Fig. 5D–F).

Then, we tested the expression of CD39 and CD73 in effector CD4 and CD8 T-cell subsets and observed that while CD8 and CD4 T cells expressed reduced level of CD73 in mCRC patients, a similar level of CD39 was observed in mCRC patients compared with healthy volunteers (Fig. 5D–F).

Together, these data demonstrate that in mCRC patients, gMDSC expressed high levels of PD-L1, CD73, and CD39, while Th1 and CD8 memory cells expressed PD-1, thus suggesting that gMDSC could blunt T-cell response using both ectonucleotidases and PD-L1.

gMDSC blunts T-cell function in a PD-L1– and ectonucleotidase-dependent manner

To test the immunosuppressive function of MDSC from mCRC patients, we sorted $CD3^+$ T cells and gMDSC and mMDSC from 5 mCRC patients. In an autologous model, we stimulated T cells with CD3 plus CD28 mAb and added in the culture either gMDSC or mMDSC in the presence of ATP molecule. As a control, we used granulocytes in this experiment. We observed that both gMDSC and mMDSC subsets have an immunosuppressive effect on T cells, demonstrated by reduced TNFα and Ki67 proliferation marker expression, however, gMDSC exert a more important immunosuppressive effect (Fig. 6A and B). Similar results were obtained using TNFα ELISA assay (Fig. 6C). Importantly, the addition of nivolumab, a clinically available anti PD-1 mAb, and/or the antagonistic anti-CD39 mAb BY40 blunted the immunosuppressive effect of gMDSC on $CD3^+$ T cells, while it did not affect the immunosuppressive effect of mMDSC (Fig. 6A–C).

Together, these data show that gMDSCs that accumulate in mCRC patients have a high immunosuppressive function that could be targeted with anti-PD-1 or anti-CD39 antibodies.

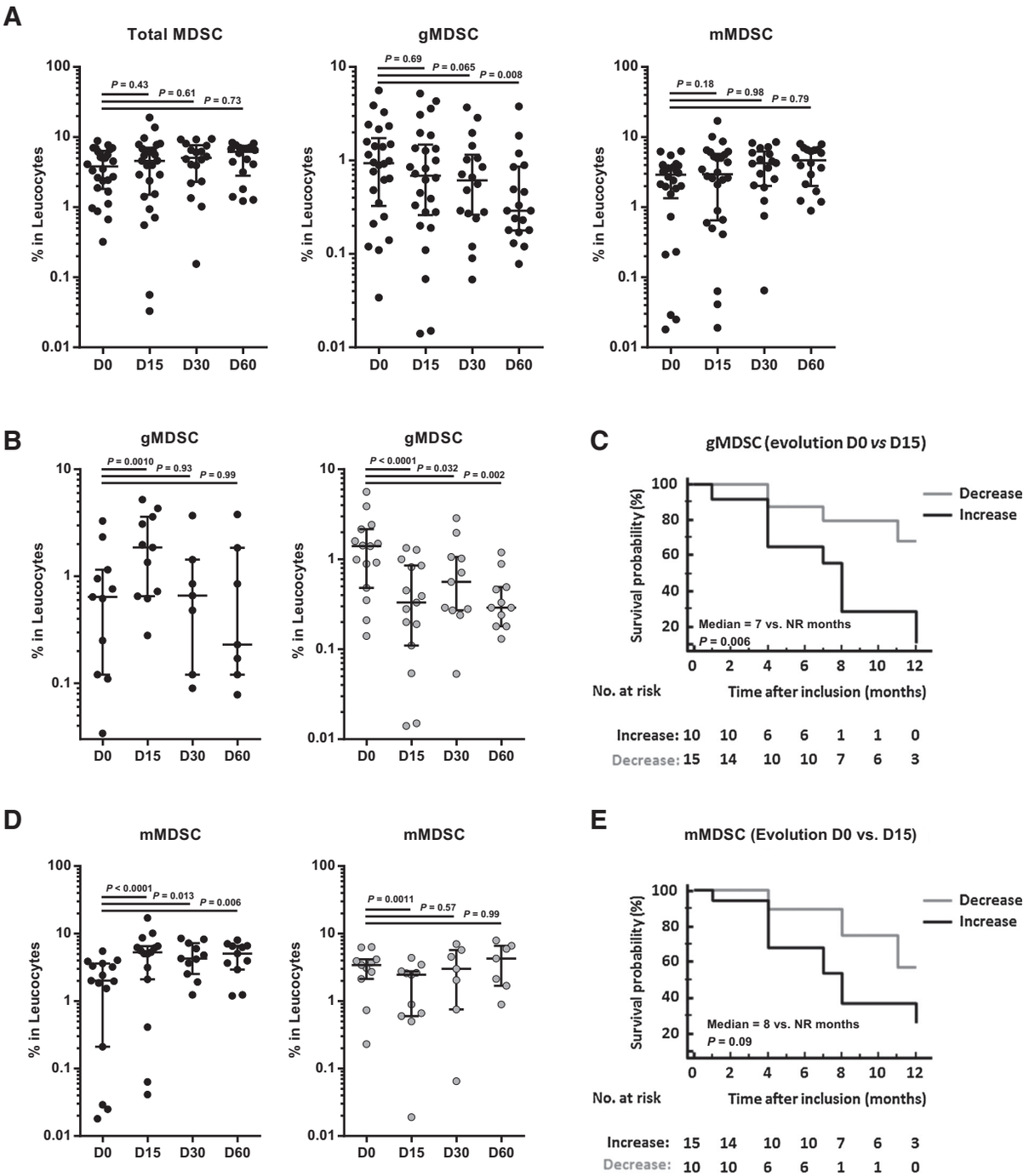

Figure 4.

Effect of FOLFOX–bevacizumab regimen on MDSCs. **A,** whole blood of mCRC patients was stained with anti-CD33, anti-Lin (i.e., anti-CD3, -CD19, -CD20, -CD56), anti-HLA-DR, anti-CD14, and anti-CD15 antibodies and was analyzed by flow cytometry before (D0) and after (D15, D30, and D60) first-line chemotherapy. The frequency of total, gMDSC or mMDSC is depicted as described in Fig. 3D and E. The data presented constitute the analysis performed on 25 mCRC patients. **B,** evolution (D0, D15, D30, and D60) of gMDSC cell frequency in the blood of a patient with an induction or a decrease of gMDSC after chemotherapy (D0 vs. D15). **C,** Kaplan–Meier curve of PFS for patients with mCRC according to the evolution (increase vs. decrease) of gMDSC cells in blood before (D0) and after (D15) chemotherapy. **D,** evolution (D0, D15, D30, and D60) of mMDSC cell frequency in the blood of a patient with an induction or a decrease of mMDSC after chemotherapy (D0 vs. D15). **E,** Kaplan–Meier curve of PFS for patients with mCRC according to the ratio (increase vs. decrease) of mMDSC cells in blood before (D0) and after (D15) chemotherapy.

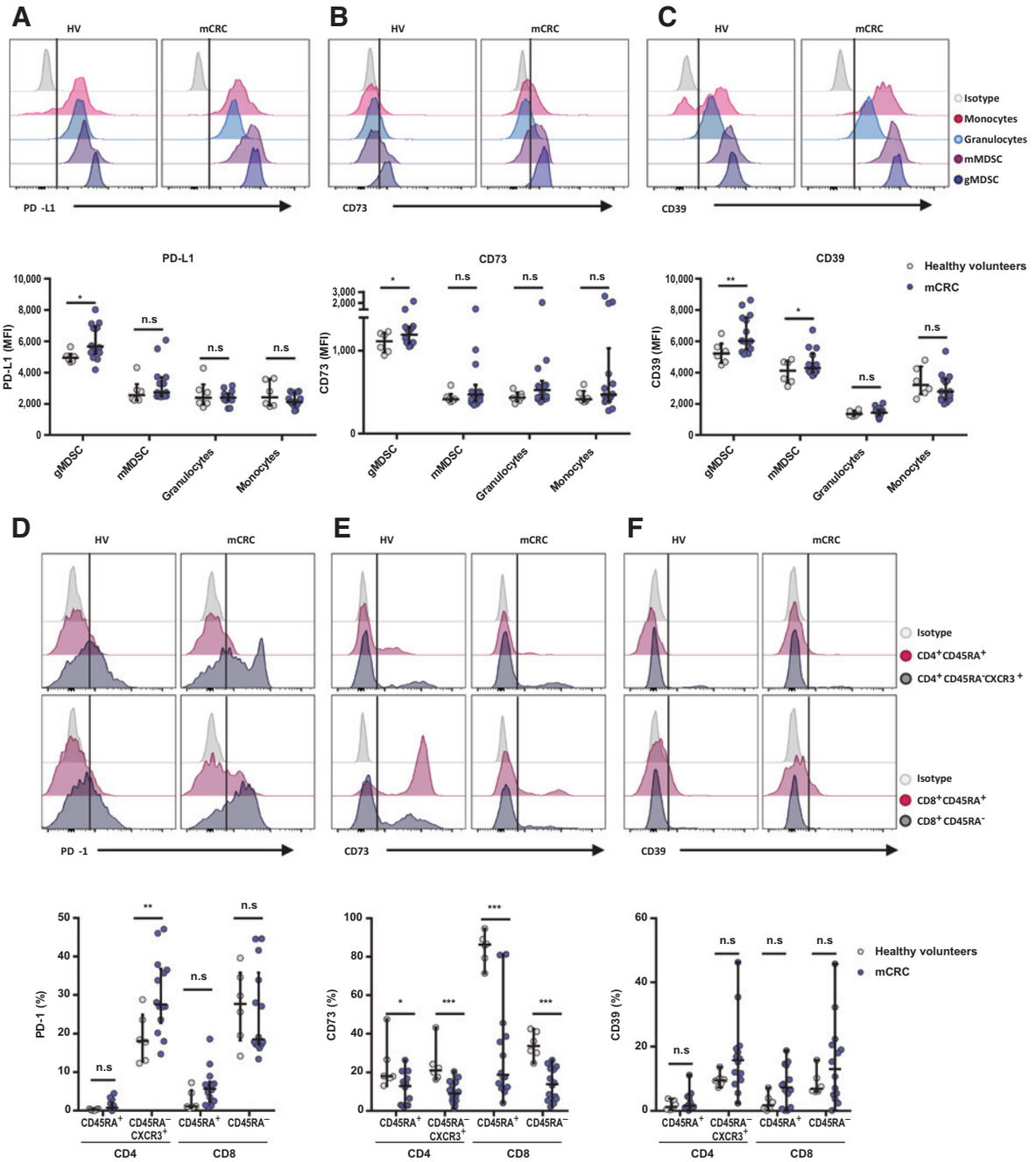

Figure 5.

MDSCs in mCRC patients express high levels of CD73, CD39, and PD-L1. **A–C,** expressions of PD-L1 (**A**), CD73 (**B**), and CD39 (**C**) on gMDSC, mMDSC, granulocytes, and monocytes are depicted. Top, representative histogram; bottom, individual data for healthy volunteers (HV; $n = 6$; gray circle) and mCRC ($n = 14$, blue circle). MFI, mean fluorescence intensity. **D–F,** expressions of PD-1 (**D**), CD73 (**E**), and CD39 (**F**) on naïve CD4 T cells, memory CXCR3$^+$ CD4 T cells, naïve CD8 T cells, and memory CD8 T cells are depicted. Top, representative histogram; bottom, individual data for healthy volunteers ($n = 6$, gray circle) and mCRC ($n = 14$, blue circle). *, $P < 0.05$; **, $P < 0.01$; ***, $P < 0.001$ (Mann-Whitney test). n.s., not significant.

Discussion

Previous reports have shown that a high number of MDSC is associated with a poor prognosis in different solid cancers and in hematologic malignancies like chronic lymphocytic leukemia or myeloma (23–25). However, the prognostic role of MDSCs has not been yet addressed in mCRC. We observed here that accumulation of gMDSC in mCRC is associated with a poor outcome. However, due to the low number of patients, further studies are required to confirm this observation and determine whether

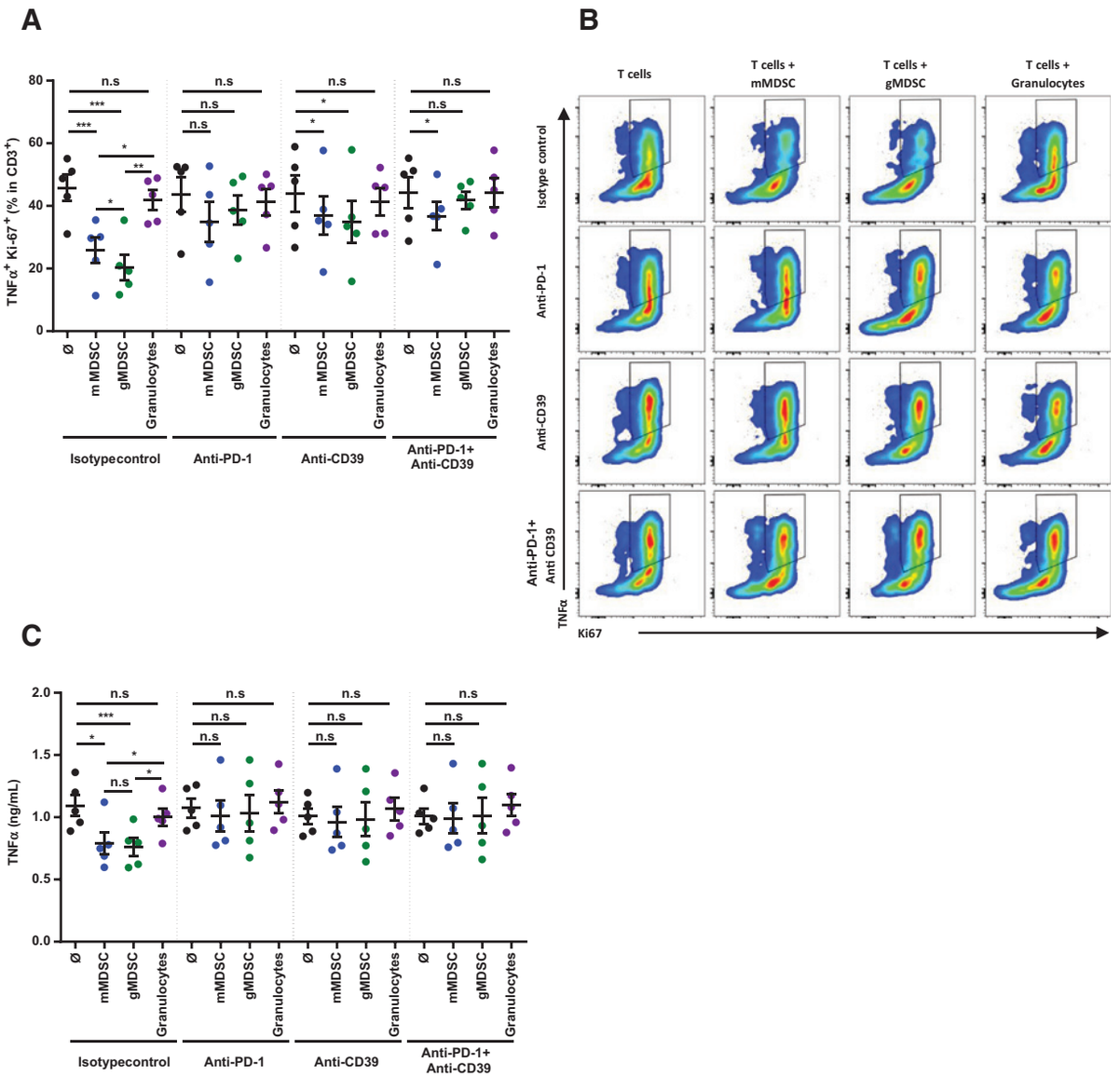

Figure 6.

gMDSC blunts T-cell function in a PD-L1– and ectonucleotidase-dependent manner. **A** and **B,** total CD3, granulocytes, mMDSC, and gMDSC subsets were sorted from a cancer patient's blood. Then, CD3 cells were activated with anti-CD3 and anti-CD28 as effector cells and cocultured with or without myeloid cells at different ratios (in the presence of ATP) for 5 days. TNFα and Ki67 expression was assessed using intracellular staining and was analyzed in $CD3^+$ T cells. One representative experiment is shown for **B** and for **A**, results are for 5 independent patients. *, $P < 0.05$; **, $P < 0.01$; ***, $P < 0.001$. **C,** TNFα secretion was assessed using ELISA on the supernatants of cocultures after 5 days. Experiment was performed as in **A**. Data are mean ± SD of three independent experiments. *, $P < 0.05$. n.s., not significant.

gMDSC accumulation is an independent prognostic factor in mCRC.

We observed that mMDSCs are the most frequent MDSC population in patient blood. Such data contrast with previous reports on MDSC in colorectal cancer, in which the authors did not observe expression of CD15 or CD14 on MDSC or only detected $CD15^+$ gMDSC (14, 21). Definition of human MDSC phenotype is still controversial. Although $CD14^+$ Lin^- $HLA\text{-}DR^-$ cells were commonly admitted to be mMDSC, the definitive of gMDSC is not consensual. Most reports define gMDSCs as low-density granulocytes copurified with PBMC during Ficoll gradient. Here, we observed that blood $CD15^+$ $CD33^{high}$ Lin^- $HLA\text{-}DR^-$ cells are immunosuppressive cells and could be called MDSC, while $CD15^+$ $CD33^{low}$ Lin^- $HLA\text{-}DR^-$ cells are not immunosuppressive and are granulocytes. Moreover, we could compare the functions of both gMDSC and mMDSC. We observed that gMDSC have a higher immunosuppressive function than mMDSC on a per cell basis. Previous data suggested that MDSC from mCRC patients have a more important immunosuppressive function compared with MDSC from

healthy donors, but the comparison of the function of gMDSC and mMDSC was not addressed (21). We found that gMDSCs have higher levels of PD-L1, CD39, and CD73 expression and exerted a stronger immunosuppressive activity than mMDSCs. Together, such data suggest that gMDSC is the major subset of MDSC involved in immunosuppression in mCRC and strengthen the rationale to combine PD-1/PD-L1 or ectonucleotidase-neutralizing antibodies with chemotherapy to blunt immunosuppression induced by gMDSC in mCRC.

In a previous report, we observed that 5-FU mediated MDSC depletion via an induction of cell death (15). In humans, a recent study on a few colorectal cancer patients treated with FOLFOX (6 patients) or FOLFIRI (4 patients) showed that while FOLFOX treatment of patients with colorectal cancer led to a decrease in MDSC levels, FOLFIRI had the opposite effect (26). In this report, we also observed that FOLFOX–bevacizumab induces a decrease of MDSC but only of the gMDSC subset. This reduction of gMDSC frequency is preferentially observed in patients with initial high level of gMDSC ($\geq$1% in leucocytes), thus raising the hypothesis that accumulating gMDSC from mCRC patients may have a specific biology that renders them more sensitive to chemotherapy-induced cell death.

We had previously reported that MDSC cell death mediated by 5-FU induced the activation of NLRP3 inflammasome and was associated with IL1β secretion. This IL1β secretion promoted induction of Th17 response. We demonstrated that Th17 induction was associated with the accumulation of proangiogenic molecules in the tumor. Such phenomenon is deleterious, and depletion of IL17A or IL1β is associated with enhanced efficacy of 5-FU treatment in mice (16). In this report, we observed that FOLFOX–bevacizumab induced Th17 accumulation after one cycle. Concomitantly, we also noted a decrease of gMDSC in patients with high initial levels. Such data strongly support that this combination of chemotherapy also affects antitumor immune response through similar mechanisms to those observed with 5-FU monotherapy in mouse and human models. Importantly, increase in Th17 cells and absence of reduction of gMDSC frequency are both associated with a poor prognosis, thus suggesting, in a similar way to mouse observations, that FOLFOX–bevacizumab induced a deleterious effect on immune response via induction of Th17 polarization.

In conclusion, our study shows that FOLFOX–bevacizumab chemotherapy induced accumulation of Th17 cells in patients, and this parameter is associated with poor prognosis, while gMDSC depletion is associated with better outcome. However, the most important point in this study is that gMDSC is an MDSC subset that could be targeted in mCRC using molecules that target the PD-1/PD-L1 or CD39/CD73 ectonucleotidase pathways. Thus, our data give rationale to use ectonucleotidase inhibitors or anti-PD-1/PD-L1 in association with FOLFOX–bevacizumab regimen in further clinical development of chemoimmunotherapy in human colorectal cancer.

Disclosure of Potential Conflicts of Interest

N. Bonnefoy is a consultant/advisory board member for OREGA Biotech. L. Apetoh is a consultant/advisory board member for Bristol-Myers Squibb. No potential conflicts of interest were disclosed by the other authors.

Authors' Contributions

Conception and design: E. Limagne, S. Ladoire, L. Apetoh, F. Ghiringhelli
Development of methodology: E. Limagne, V. Derangère, F. Végran, S. Ladoire
Acquisition of data (provided animals, acquired and managed patients, provided facilities, etc.): E. Limagne, R. Euvrard, M. Thibaudin, N. Bonnefoy, J. Vincent, L. Bengrine-Lefevre
Analysis and interpretation of data (e.g., statistical analysis, biostatistics, computational analysis): E. Limagne, R. Euvrard, M. Thibaudin, V. Derangère, R. Boidot, L. Apetoh, F. Ghiringhelli
Writing, review, and/or revision of the manuscript: E. Limagne, R. Euvrard, M. Thibaudin, C. Rébé, V. Derangère, F. Végran, N. Bonnefoy, D. Delmas, L. Apetoh, F. Ghiringhelli
Administrative, technical, or material support (i.e., reporting or organizing data, constructing databases): C. Rébé, A. Chevriaux, R. Boidot, S. Ladoire
Study supervision: E. Limagne, L. Apetoh, F. Ghiringhelli

Acknowledgments

We thank Aurelie Bertaut (statistician) for calculation of the required number of patients.

Grant Support

This work was supported by the Ligue Nationale contre le Cancer, the Institut National du Cancer, the Association pour la recherche sur le cancer, the Conseil Régional Bourgogne/INSERM, Fondation pour la Recherche Médicale (F. Ghiringhelli) the Fondation de France, the Fondation Lilliane Betancourt, the French National Research Agency (ANR-13-JSV3-0001 and ANR-11-LABX-0021), the Ligue Régionale contre le Cancer Comité Grand-Est, the Canceropôle Grand-Est, and the European Community (Marie Curie Fellowship PCIG10-GA-2011-303719 to L. Apetoh). This work was also supported by institutional grants from INSERM and Université de Montpellier 1 and from the LabEx MabImprove (N. Bonnefoy).

The costs of publication of this article were defrayed in part by the payment of page charges. This article must therefore be hereby marked *advertisement* in accordance with 18 U.S.C. Section 1734 solely to indicate this fact.

Received November 17, 2015; revised June 2, 2016; accepted July 5, 2016; published OnlineFirst August 5, 2016.

References

1. Principi M, Barone M, Pricci M, De Tullio N, Losurdo G, Ierardi E, et al. Ulcerative colitis: from inflammation to cancer. Do estrogen receptors have a role? World J Gastroenterol 2014;20:11496–04.
2. Galon J, Costes A, Sanchez-Cabo F, Kirilovsky A, Mlecnik B, Lagorce-Pagès C, et al. Type, density, and location of immune cells within human colorectal tumors predict clinical outcome. Science 2006;313:1960–64.
3. Pagès F, Berger A, Camus M, Sanchez-Cabo F, Costes A, Molidor R, et al. Effector memory T cells, early metastasis, and survival in colorectal cancer. The N Engl J Med 2005;353:2654–66.
4. Salama P, Stewart C, Forrest C, Platell C, Iacopetta B. FOXP3+ cell density in lymphoid follicles from histologically normal mucosa is a strong prognostic factor in early stage colon cancer. Cancer Immunol Immunother 2012;61:1183–90.
5. Bindea G, Mlecnik B, Tosolini M, Kirilovsky A, Waldner M, Obenauf AC, et al. Spatiotemporal dynamics of intratumoral immune cells reveal the immune landscape in human cancer. Immunity 2013;39:782–95.
6. Mei Z, Liu Y, Liu C, Cui A, Liang Z, Wang G, et al. Tumour-infiltrating inflammation and prognosis in colorectal cancer: systematic review and meta-analysis. Br J Cancer 2014;110:1595–605.
7. Salama P, Phillips M, Grieu F, Morris M, Zeps N, Joseph D, et al. Tumor-infiltrating FOXP3+ T regulatory cells show strong prognostic significance in colorectal cancer. J Clin Oncol 2009;27:186–92.
8. Liu J, Duan Y, Cheng X, Chen X, Xie W, Long H, et al. et al.IL-17 is associated with poor prognosis and promotes angiogenesis via stimulating VEGF production of cancer cells in colorectal carcinoma. Biochem Biophys Res Commun 2011;407:348–54.

9. Chung AS, Wu X, Zhuang G, Ngu H, Kasman I, Zhang J, et al. An interleukin-17-mediated paracrine network promotes tumor resistance to anti-angiogenic therapy. Nat Med 2013;19:1114–23.
10. Apetoh L, Vegran F, Ladoire S, Ghiringhelli F. Restoration of antitumor immunity through selective inhibition of myeloid derived suppressor cells by anticancer therapies. Curr Mol Med 2011;11:365–72.
11. Marvel D, Gabrilovich DI. Myeloid-derived suppressor cells in the tumor microenvironment: expect the unexpected. J Clin Invest 2015; 125:3356–64.
12. Gabrilovich DI, Ostrand-Rosenberg S, Bronte V. Coordinated regulation of myeloid cells by tumours. Nat Rev Immunol 2012;12:253–68.
13. Solito S, Marigo I, Pinton L, Damuzzo V, Mandruzzato S, et al. Myeloid-derived suppressor cell heterogeneity in human cancers. Ann N Y Acad Sci 2014;1319:47–65.
14. OuYang LY, Wu XJ, Ye SB, Zhang RX, Li ZL, Liao W, et al. et al.Tumor-induced myeloid-derived suppressor cells promote tumor progression through oxidative metabolism in human colorectal cancer. J Transl Med 2015;13:47.
15. Vincent J, Mignot G, Chalmin F, Ladoire S, Bruchard M, Chevriaux A, et al. 5-Fluorouracil selectively kills tumor-associated myeloid-derived suppressor cells resulting in enhanced T cell-dependent antitumor immunity. Cancer Res 2010;70:3052–61.
16. Bruchard M, Mignot G, Derangère V, Chalmin F, Chevriaux A, Végran F, et al. Chemotherapy-triggered cathepsin B release in myeloid-derived suppressor cells activates the Nlrp3 inflammasome and promotes tumor growth. Nat Med 2013;19:57–64.
17. Eisenhauer EA, Therasse P, Bogaerts J, Schwartz LH, Sargent D, Ford R, et al. New response evaluation criteria in solid tumours: revised RECIST guideline (version 1.1). Eur J Cancer 2009;45:228–47.
18. McCleary NJ, Meyerhardt JA, Green E, Yothers G, de Gramont A, Van Cutsem E, et al. Impact of age on the efficacy of newer adjuvant therapies in patients with stage II/III colon cancer: findings from the ACCENT database. J Clin Oncol 2013;31:2600–6.
19. Mahnke YD, Roederer M. Optimizing a multicolor immunophenotyping assay. Clin Lab Med 2007;27:469–85.
20. Tesniere A, Apetoh L, Ghiringhelli F, Joza N, Panaretakis T, Kepp O, et al. Immunogenic cancer cell death: a key-lock paradigm. Curr Opin Immunol 2008;20:504–11.
21. Zhang B, Wang Z, Wu L, Zhang M, Li W, Ding J, et al. Circulating and tumor-infiltrating myeloid-derived suppressor cells in patients with colorectal carcinoma. PLoS One 2013;8:e57114.
22. Bastid J, Cottalorda-Regairaz A, Alberici G, Bonnefoy N, Eliaou JF, Bensussan A. ENTPD1/CD39 is a promising therapeutic target in oncology. Oncogene 2013;32:1743–51.
23. Chen MF, Kuan FC, Yen TC, Lu MS, Lin PY, Chung YH, et al. et al.IL-6-stimulated CD11b+ CD14+ HLA-DR- myeloid-derived suppressor cells, are associated with progression and poor prognosis in squamous cell carcinoma of the esophagus. Oncotarget 2014;5: 8716–28.
24. Idorn M, Kollgaard T, Kongsted P, Sengelov L, Thor Straten P. Correlation between frequencies of blood monocytic myeloid-derived suppressor cells, regulatory T cells and negative prognostic markers in patients with castration-resistant metastatic prostate cancer. Cancer Immunol Immunother 2014;63:1177–87.
25. Romano A, Parrinello NL, Vetro C, Forte S, Chiarenza A, Figuera A, et al. Circulating myeloid-derived suppressor cells correlate with clinical outcome in Hodgkin lymphoma patients treated up-front with a risk-adapted strategy. Br J Haematol 2015;168:689–700.
26. Kanterman J, Sade-Feldman M, Biton M, Ish-Shalom E, Lasry A, Goldshtein A, et al. et al.Adverse immunoregulatory effects of 5FU and CPT11 chemotherapy on myeloid-derived suppressor cells and colorectal cancer outcomes. Cancer Res 2014;74:6022–35.